Real-time completion monitoring of deepwater wells: Part III – Comparison of experiments and modeling

Andrey Bakulin, formerly Shell International E & P Inc, presently WesternGeco/Schlumberger; Dmitry Alexandrov*, Alexander Sidorov, Boris Kashtan, St. Petersburg State University; Mikko Jaaskelainen, formerly Shell International E & P Inc, presently SensorTran.

Summary

Real-time completion monitoring (RTCM) with acoustic waves has recently been proposed as a method to monitor permeability changes along the completions. Typical deepwater completions contain additional layers of sand screen, gravel sand, and perforated casing which make them quite different from a fluid-filled open borehole. Monitoring changes of flow properties across the completion is crucial since impairment of permeability in any of these layers could cause reduced well productivity. In contrast to open-hole model, sand-screened completion supports two tube waves related to inner fluid column and gravel suspension in the annulus. We construct simple numerical models of various completion scenarios using poroelastic description of screen and sand. Despite limitations, such models provide qualitative and sometimes semi-quantitative description to the laboratory experiments with full-scale model of horizontal well.

Introduction

Real-time completion monitoring was proposed by Bakulin et al (2008a,b, 2009) as a method to detect impairment (permeability reduction) changes along the deepwater completions using tube-wave signatures. Bakulin et al (2008a,b) hypothesized that gravel sand should have small but non-zero shear velocity. In this case only single tube wave exists with properties that are affected by all completion layers. However actual experiments with sand-screened completions (Bakulin et al, 2009) revealed two clear tube-wave arrivals, thus suggesting that perhaps gravel sand has negligible shear velocity and acts largely as a fluid suspension. This was an important experimental finding since completion with two fluid columns (fluid inside the screen and gravel sand suspension in the annulus) supports two tube waves similar to an earlier model and experiments without gravel pack. In this study we attempt a more systematic analysis of tube-wave signatures based on experimental data in gravel-packed completions with realistic wire-wrapped sand screens. We also attempt to generalize our simple analytical model to describe these signatures taking into account the permeable nature of gravel pack and sand screen.

Sand-screened completion without gravel pack

Let us consider an idealized model of sand-screened completion with a free outer boundary (air) as used in the reported experiments (Bakulin et al, 2008a,b, 2009): fluid – permeable screen – fluid – casing. Following previous studies we model the sand screen as a layer of poroelastic Biot material. At low frequencies such model supports two tube waves and two plate (extensional) waves. Figure 1a shows seismograms for such case where fast and slow tube waves propagate without attenuation. To compare with the experimental results all synthetic data shows a radial component of displacement on the boundary of the outer pipe (casing) as this is the quantity measured by the fiber-optic sensors (Bakulin et al, 2009).
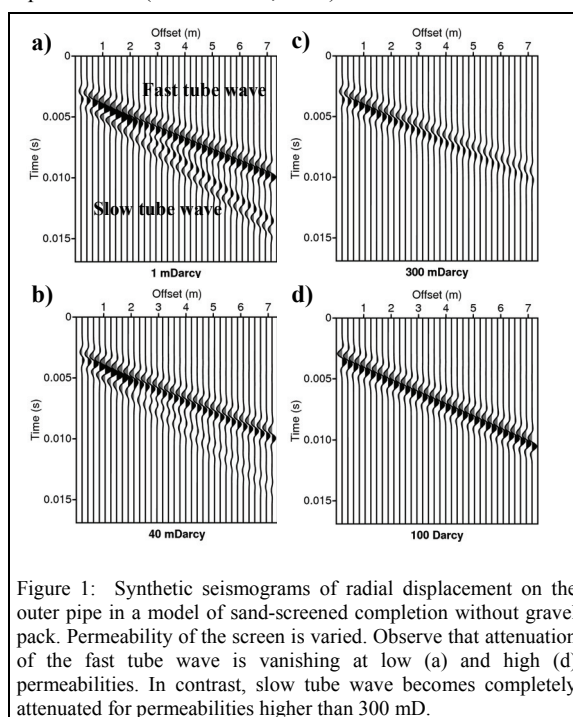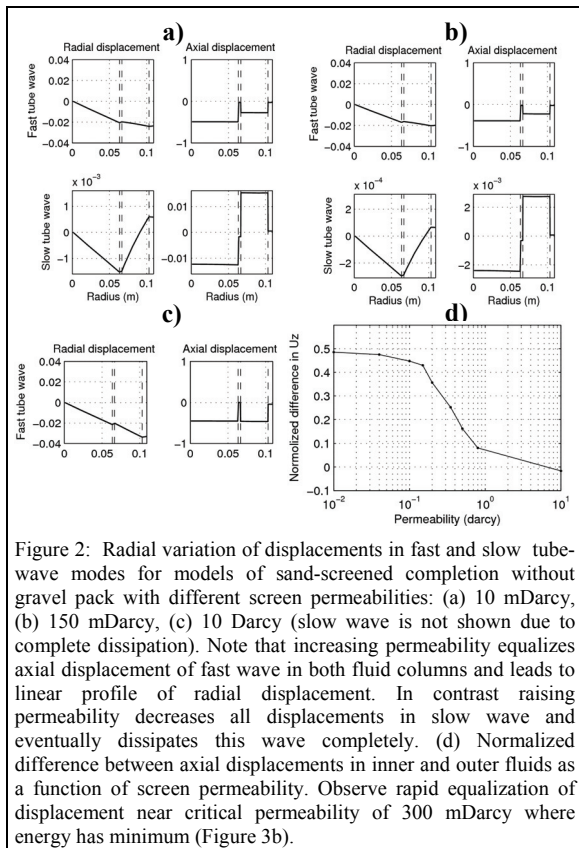

Figure 1: Synthetic seismograms of radial displacement on the outer pipe in a model of sand-screened completion without gravel pack. Permeability of the screen is varied. Observe that attenuation of the fast tube wave is vanishing at low (a) and high (d) permeabilities. In contrast, slow tube wave becomes completely attenuated for permeabilities higher than 300 mD.

To understand the nature of tube-wave modes it is instructive to analyze radial distribution of displacements for each mode (Figure 2a). There is a remarkable difference between two tube-wave modes: fast tube wave has displacements of the same sign inside both fluid columns, whereas slow wave has displacements of opposite signs. Fast wave is the one that transforms to a regular tube wave when shear rigidity of the inner pipe goes to zero. Therefore we can interpret that the fast wave is supported by the outer pipe, whereas the slow one is supported by the inner pipe as originally proposed by Bakulin et al (2008a).

When the screen permeability increases, then both waves start to attenuate (Figure 1b-c), however their dependence on permeability is quite different. To obtain simple first-order dependence on permeability, we use attributes derived from slowness-frequency and velocity spectra (Bakulin et al, 2008a). Velocity is estimated as a speed where maximum energy is achieved on velocity spectra (averaged for all frequencies). Energy attribute simply denote value of the peak for the wave of interest. Normalization is performed with respect to the base case of the impermeable screen.

Figure 2: Radial variation of displacements in fast and slow tube-wave modes for models of sand-screened completion without gravel pack with different screen permeabilities: (a) 10 mDarcy, (b) 150 mDarcy, (c) 10 Darcy (slow wave is not shown due to complete dissipation). Note that increasing permeability equalizes axial displacement of fast wave in both fluid columns and leads to linear profile of radial displacement. In contrast raising permeability decreases all displacements in slow wave and eventually dissipates this wave completely. (d) Normalized difference between axial displacements in inner and outer fluids as a function of screen permeability. Observe rapid equalization of displacement near critical permeability of 300 mDarcy where energy has minimum (Figure 3b).

Varying screen permeability from 0 Darcy to 1000 Darcy we obtain Figure 3. Vanishing permeability makes the poroelastic screen to become equivalent to an elastic impermeable solid for which both waves should have no attenuation. At the other extreme, a screen with a very large permeability is similar to a layer of fluid. It becomes so permeable that it provides almost no resistance to the radial fluid motion across the screen. Since the fast tube wave is supported by the outer casing it exhibits no attenuation and dispersion as it should in a liquid-filled cylinder. In

contrast, the slow wave, supported by the inner pipe, totally disappears since the screen does not provide any resistance to the radial motion of the fluid to maintain this arrival.
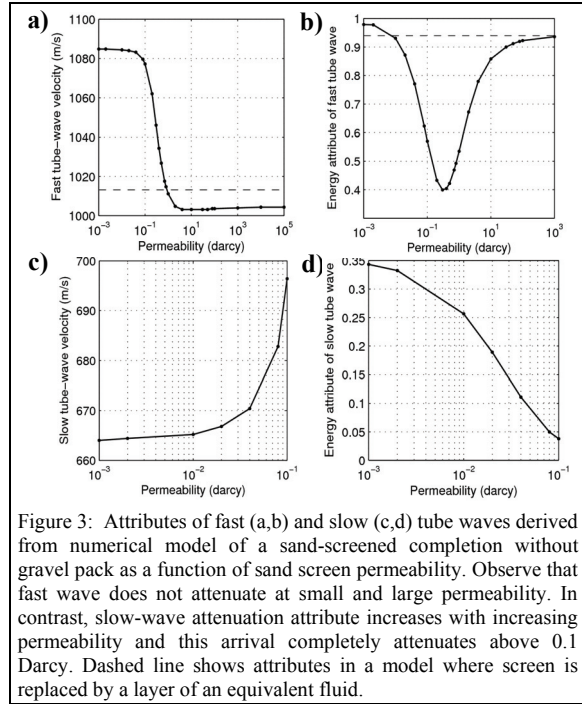

Figure 3: Attributes of fast (a,b) and slow (c,d) tube waves derived from numerical model of a sand-screened completion without gravel pack as a function of sand screen permeability. Observe that fast wave does not attenuate at small and large permeability. In contrast, slow-wave attenuation attribute increases with increasing permeability and this arrival completely attenuates above 0.1 Darcy. Dashed line shows attributes in a model where screen is replaced by a layer of an equivalent fluid.

At intermediate values of permeabilities the slow tube wave experiences monotonic increase in attenuation with increase in permeability and becomes almost unobservable (as a separate peak) at permeabilities larger than 0.1 Darcy.

This can be readily explained by radial profiles of displacement for this mode (Figure 2). The slow tube wave is analogous to a slow Biot wave in a sense that it has opposite signs of displacement in two fluid columns. As one can see on Figure 2a first arrivals in inner fluid has negative axial displacement, whereas in inner fluid axial displacement is of opposite sign. When the screen becomes permeable, fluid on both sides starts to communicate and this motion leads to strong attenuation that eventually completely absorbs this wave (Figure 2b). In contrast, fast wave has maximum attenuation at about 300 mDarcy and then returns to the state of virtually no attenuation at large permeability (Figure 3b). Radial profiles provide an additional insight on possible mechanism of this attenuation at intermediate permeabilities. For low permeabilities axial displacements of the fast wave are of the same sign, but of different magnitudes (Figure 2a). When screen becomes permeable these different rates of compression inside two liquid columns lead to a fluid exchange across the screen. This exchange particularly intensifies near 300 mDarcy which is manifested by rapid

equalization of axial displacements occurring in this region (Figure 2d). At high permeabilities axial displacements become equal (Figure 2c), whereas radial displacement resembles linear profile typical for conventional tube wave.

Let us compare predictions of this simple model with the experimental data. Figure 4a shows experimental seismograms for a blank pipe that simulates an impermeable screen. Similar to modeling, two arrivals are recognizable with velocities ~ 1000 m/s and 700 m/s. In the presence of an open to flow wire-wrapped screen, acoustic response changes substantially (Figure 4b). Let us review which numerical predictions are in agreement and disagreement with the experiment. First, Figure 4b has an amplitude level similar to that of Figure 4a. This is in agreement with predictions from Figure 3b suggesting that open to flow sand screens (~250-1000 Darcy) should lead to small energy loss in fast tube waves. Second, Figure 3a predicts reduction in velocity of the fast wave, which is also seen in the experiment albeit to a larger extent. There are also disagreements between modeling and experiment in particular what concerns behavior of slow tube wave. First, modeling suggests that this arrival is fully attenuated at permeabilities larger than 0.1 Darcy (Figure 3d). However experimental data (Figure 4b) clearly shows low-frequency slow arrival. Second, velocities of both fast and slow arrivals are substantially lower in the experiment. We conclude that experimental data suggest that such simplistic poroelastic modeling of sand screens is clearly deficient especially as far as slow tube wave is concerned.
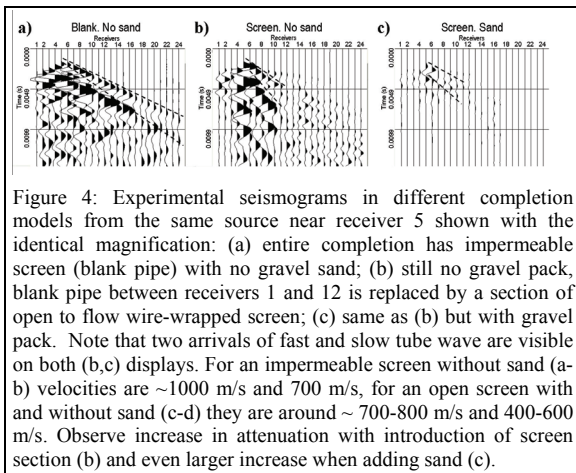

Figure 4: Experimental seismograms in different completion models from the same source near receiver 5 shown with the identical magnification: (a) entire completion has impermeable screen (blank pipe) with no gravel sand; (b) still no gravel pack, blank pipe between receivers 1 and 12 is replaced by a section of open to flow wire-wrapped screen; (c) same as (b) but with gravel pack. Note that two arrivals of fast and slow tube wave are visible on both (b,c) displays. For an impermeable screen without sand (a-b) velocities are ~1000 m/s and 700 m/s, for an open screen with and without sand (c-d) they are around ~ 700-800 m/s and 400-600 m/s. Observe increase in attenuation with introduction of screen section (b) and even larger increase when adding sand (c).

Sand-screened completion with gravel pack
Figure 5 shows energy and velocity attributes as a function of gravel sand permeability for a model with gravel-packed completion when the sand screen is completely impermeable. We observe that in the limit of small and large permeabilities energy of fast and slow tube waves

does not attenuate which can be given a following physical interpretation. When the permeability is very low, fluid and solid phases of the sand should move in synchrony and simulate effective fluid because of zero shear rigidity of the frame. Both energy and velocity attributes match quite well with their counterparts for a model with sand replaced by an equivalent fluid. For very large permeability, the fluid phase can freely move through the gravel layer and also be close to the behavior of lossless fluid albeit with slightly
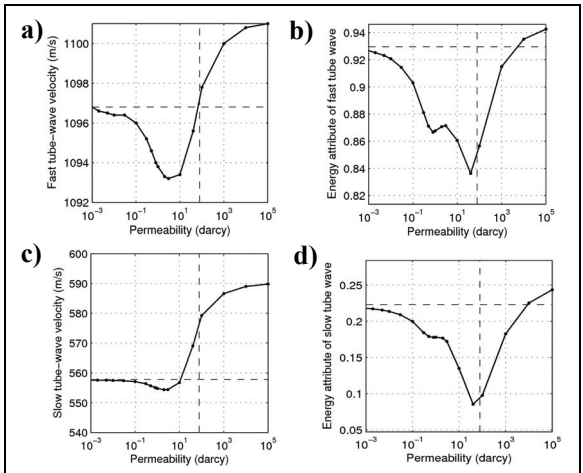

Figure 5: Attributes of fast (a,b) and slow (c,d) tube waves derived from numerical model of gravel-packed sand-screened completion with an impermeable screen (0 Darcy) as a function of gravel sand permeability. Note large effects of gravel sand permeability on tube-wave signatures despite the fact that both screen and casing are impermeable.
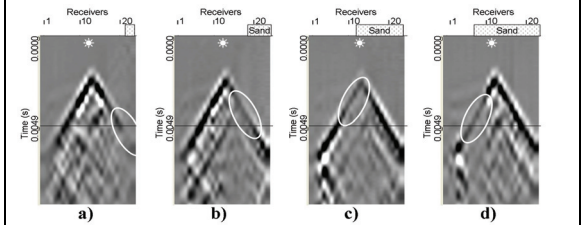

Figure 6: Experimental acoustic responses in a model of a completion with blank pipe at various consecutive stages of gravel packing process. Sand is injected from the right side. Part of the model with maximum gravel packing is shown by dashed box. Part of the model to the left of the box contains some limited amount of gravel. Observe dim spot anomaly associated with the partially packed part.

different velocities. At intermediate permeabilities the relative fluid motion in the pores leads to substantial attenuation of both arrivals, and in particular to that of the slow tube wave (Figure 5d). It is interesting to see that location of the maximum attenuation is close to the permeability at which the Biot critical frequency is roughly equal to the central frequency of the source signal (Figure

5, vertical dashed line). In the experiments we did not vary the permeability of the gravel sand. However we conducted acoustic measurements during the entire gravel packing process. One such experiment consisted in gravel packing of the blank pipe (Bakulin et al, 2009). Before packing we have the annulus filled with water of infinite permeability. At the end of the gravel packing we have the annulus full of gravel sand with permeability ~ 200-300 Darcy. Let us make the assumption that a combination of gravel and water layers spans the range of permeabilities from infinity to 200 Darcy during the entire gravel packing process. Thus we can compare the conducted experiment to the theoretical model with varying permeability of the sand in the annulus (Figure 5). Figure 6 presents experimental data at four different times during various stages of the gravel packing process. The extent of the model where maximum packing has been reached is shown by dotted box above the plots. Ahead of this large front we have a sand layer of a smaller height. One can clearly observe that a dim amplitude anomaly is moving across the model ahead of the front with maximum packing. Once the pack is in place this anomaly is gone. We observe a good match between theoretical predictions and experimental data. There are very similar attenuation and velocities in extreme cases of water- and gravel-sand annulus (Figure 6). This is consistent with prediction from modeling for large and small permeabilities (Figure 5b,d). Somewhere between those limiting values of water (infinite) and sand permeability (200 Darcy) we hit that "critical permeability" with maximum attenuation and observe low amplitudes (dim anomaly) of both arrivals (Figure 6). Likewise, modeling predicts an energy trough for both the fast and slow waves (Figure 5b,d). Experimental data suggests that "critical permeability" is somewhere above 200 Darcy, whereas the model predicts it at ~ 80 Darcy. Despite factor of two or more discrepancy these estimates are in reasonable agreement after noting that numerical model is axisymmetric whereas actual model is stratified 3D.

Figure 7 shows predicted velocities and energy attributes for a gravel-packed completion with open sand screen (100 Darcy). At very low permeabilities we observe no attenuation. When permeability increases a fluid exchange becomes increasingly possible, thus introducing a large attenuation of the fast wave and completely absorbing the slow wave. In the limit of very large permeability both sand and screen form a very permeable layer that behaves similar to a layer of fluid. Thus we observe no attenuation of the fast wave, while the slow wave is absent similar to the case when the screen is replaced by a fluid layer.
Experiments show that most notable impact of the gravel sand is strong attenuation of both modes and in particular of a slow mode (Figure 4b,c). Comparing such behavior with the model from Figure 7 we observe following similarities. Without gravel pack annulus is filled with water (infinite permeability). This can be likened to a gravel pack of very high permeability which should have little attenuation (Figure 7b). Experimental plot 4b confirms this expectation and verifies that relatively small attenuation is observed with respect to a reference case of blank pipe (Figure 4a). In contrast, replacing water with sand reduces permeability from infinity to ~ 200 Darcy which can be approximated as moving from high to medium permeabilities on Figure 7b. At those intermediate permeabilities we observe greatly increased attenuation of the fast wave which is in qualitative agreement with the experiment.
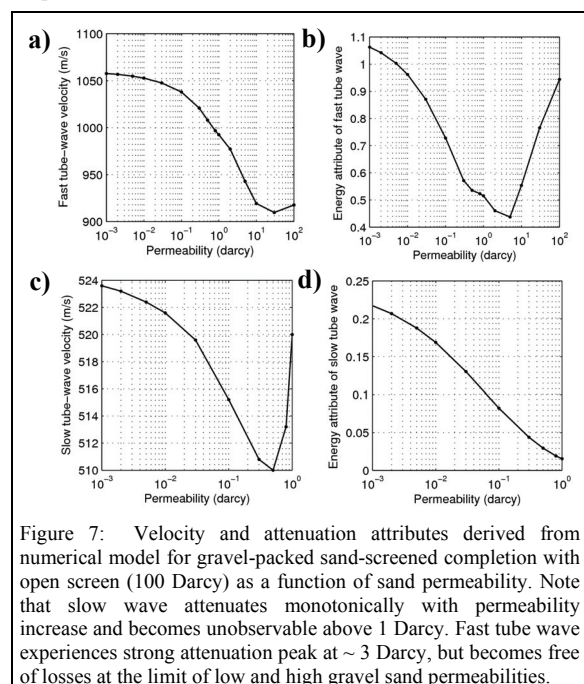

Figure 7: Velocity and attenuation attributes derived from numerical model for gravel-packed sand-screened completion with open screen (100 Darcy) as a function of sand permeability. Note that slow wave attenuates monotonically with permeability increase and becomes unobservable above 1 Darcy. Fast tube wave experiences strong attenuation peak at ~ 3 Darcy, but becomes free of losses at the limit of low and high gravel sand permeabilities.

Summary and outlook
We examined borehole wave propagation in sand-screened gravel-packed deepwater completions based on full-scale laboratory experiments and poroelastic numerical modeling. Both experiments and models confirm that at low frequencies propagation is dominated by fast and slow tube waves supported by columns of inner fluid and gravel sand suspension. Velocities and in particular attenuations of two arrivals are strongly influenced by the permeability of the sand screen and gravel pack. We build several numerical models of various completion scenarios by utilizing poroelastic description for screen and sand and study effect of screen and gravel sand permeability on the tube-wave signatures. While semi-quantitative agreement has been observed, we conclude that a better model of sand screens is required to explain the experimental data.

EDITED REFERENCES
Note: This reference list is a copy-edited version of the reference list submitted by the author. Reference lists for the 2009 SEG Technical Program Expanded Abstracts have been copy edited so that references provided with the online metadata for each paper will achieve a high degree of linking to cited sources that appear on the Web.

REFERENCES
Bakulin, A., A. Sidorov, B. Kashtan, and M. Jaaskelainen, 2008a, Real-time completion monitoring with acoustic waves: Geophysics, **73**, no. 1, E15–E33.
———, 2008b, Real-time completion monitoring of deepwater wells: Part 1—Modeling and first experiments: 78th Annual International Meeting, SEG, Expanded Abstracts, 2726–2729.
Bakulin, A., A. Sidorov, B. Kashtan, D. Alexandrov, and M. Jaaskelainen, 2009, Real-time completion monitoring of deepwater wells: Part 2—Active and passive surveillance: 79th Annual International Meeting, SEG, Expanded Abstracts.